Rift asymmetry and continental uplift

Carlo Doglioni, Eugenio Carminati, and Enrico Bonatti

Dipartimento Scienze della Terra, Università La Sapienza, Rome, Italy

[1] The topography of ocean ridges and rifts show a distinct asymmetry. The eastern sides of the East Pacific Rise, the Mid-Atlantic Ridge, and the NW Indian Ridge are, on average, 100–300 m more elevated than the conjugate flank to the west. The asymmetry is maintained when bathymetry is plotted versus the square root of crustal age. A comparable topographic asymmetry occurs in the Red Sea and Baikal rifts where the "eastern" continental shoulders are more elevated. We suggest that depleted and lighter asthenosphere generated below the ocean ridge was shifted "eastward" relative to the lithosphere, determining a density deficit below the eastern flank. The eastward migration of the lighter Atlantic asthenosphere below the African continent could eventually have contributed to the anomalous postrift uplift of Africa. This model suggests that the "westward" drift of the lithosphere relative to the underlying mantle might be a global phenomenon. *INDEX TERMS:* 8155 Tectonophysics: Plate motions—general; 8120 Tectonophysics: Dynamics of lithosphere and mantle—general; 8109 Tectonophysics: Continental tectonics—extensional (0905); 8150 Tectonophysics: Plate boundary—general (3040); 9305 Information Related to Geographic Region: Africa; *KEYWORDS:* rift asymmetry, bathymetry, lithosphere, asthenosphere, westward drift, continental uplift. **Citation:** Doglioni, C., E. Carminati, and E. Bonatti, Rift asymmetry and continental uplift, *Tectonics*, *22*(3), 1024, doi:10.1029/2002TC001459, 2003.

1. Introduction

[2] Since plate tectonics were confirmed by the recognition of specular magnetic anomalies in the two sides of oceanic ridges [*Vine and Matthews*, 1963], oceanic rift zones have in general been considered as symmetric features. The first-order bathymetry of the oceans has been related to subsidence generated by thermal contraction of the lithosphere [*Parsons and Sclater*, 1977; *Stein and Stein*, 1992; *Carlson and Johnson*, 1994]. Flattened oceanic bathymetric profiles have been related to radiogenic heating in convecting mantle [*Jarvis and Peltier*, 1980] or asthenospheric flow [*Phipps Morgan and Smith*, 1992]. However, *Calcagno and Cazenave* [1994] have shown how the subsidence of the seafloor is more complex than predicted by global plate or half-space cooling models. Petrologic, density and bathymetrical variations in

the generation of the 0–100 Ma oceanic crust have been observed [*Humler et al.*, 1999]. Initially shallow ridges subsided faster than deep ridges [*Calcagno and Cazenave*, 1994]. Basalt chemistry, axial depth and thickness of the oceanic crust [*Klein and Langmuir*, 1987] are related to the degree of melting of the underlying mantle [*Bonatti et al.*, 1993].

[3] Recent observations indicate that the symmetry across oceanic ridges is much less ubiquitous than originally thought: *Hayes* [1988], *Marty and Cazenave* [1989], *Kane and Hayes* [1992], *Calcagno and Cazenave* [1994], *Marks and Stock* [1994], and *Perrot et al.* [1998] have shown significant variations in bathymetry and subsidence rates between the conjugated oceanic flanks both in the Atlantic and in the Pacific. According to *Calcagno and Cazenave* [1994] the eastern Atlantic subsided $\sim$60 m $Myr^{-1/2}$ slower than the western Atlantic, a value significantly larger than average uncertainties in subsidence rate estimates. Looking at the seafloor age map [*Müller et al.*, 1997], asymmetric rates of spreading are evident all over the oceans, and frequently faster rates are in the eastern or northeastern plate. As a general trend, the eastern flank of oceanic ridges subsided more slowly, but there are along-axis variations of even larger magnitude [*Marty and Cazenave*, 1989].

[4] Along rift axis variations and asymmetric subsidence rates have been ascribed to presence of hotter than normal asthenosphere, which may perturb the cooling process of the plate [*Calcagno and Cazenave*, 1994]. Another model [*Phipps Morgan and Smith*, 1992] predicts an asthenospheric flow where either shallower or deeper seafloor than the half-space values depend on whether lithospheric plates are bounded by trenches or continents.

[5] Asymmetric rifting was proposed and interpreted as related to simple shear extension particularly in continental lithosphere [*Wernicke*, 1981, 1985]. Peculiar asymmetries characterize topography, gravity and geology of subduction zones as a function of their direction [*Harabaglia and Doglioni*, 1998; *Doglioni et al.*, 1999a].

[6] Here we test whether asymmetry occurs also along oceanic ridges and continental rifts, and if this asymmetry has a constant geographic polarity. We show how both oceanic and continental rift zones are generally more elevated in the eastern side, and we propose an explanation related to horizontal motion of the mantle, eventually producing continental uplift. An additional ingredient in rift zones modeling is combining the asymmetric vertical motions with the mean "eastward" relative mantle flow implicit in the "westward" drift of the lithosphere [*Bostrom*, 1971; *O'Connell et al.*, 1991; *Ricard et al.*, 1991], a concept that implies decoupling between mantle and lithosphere.
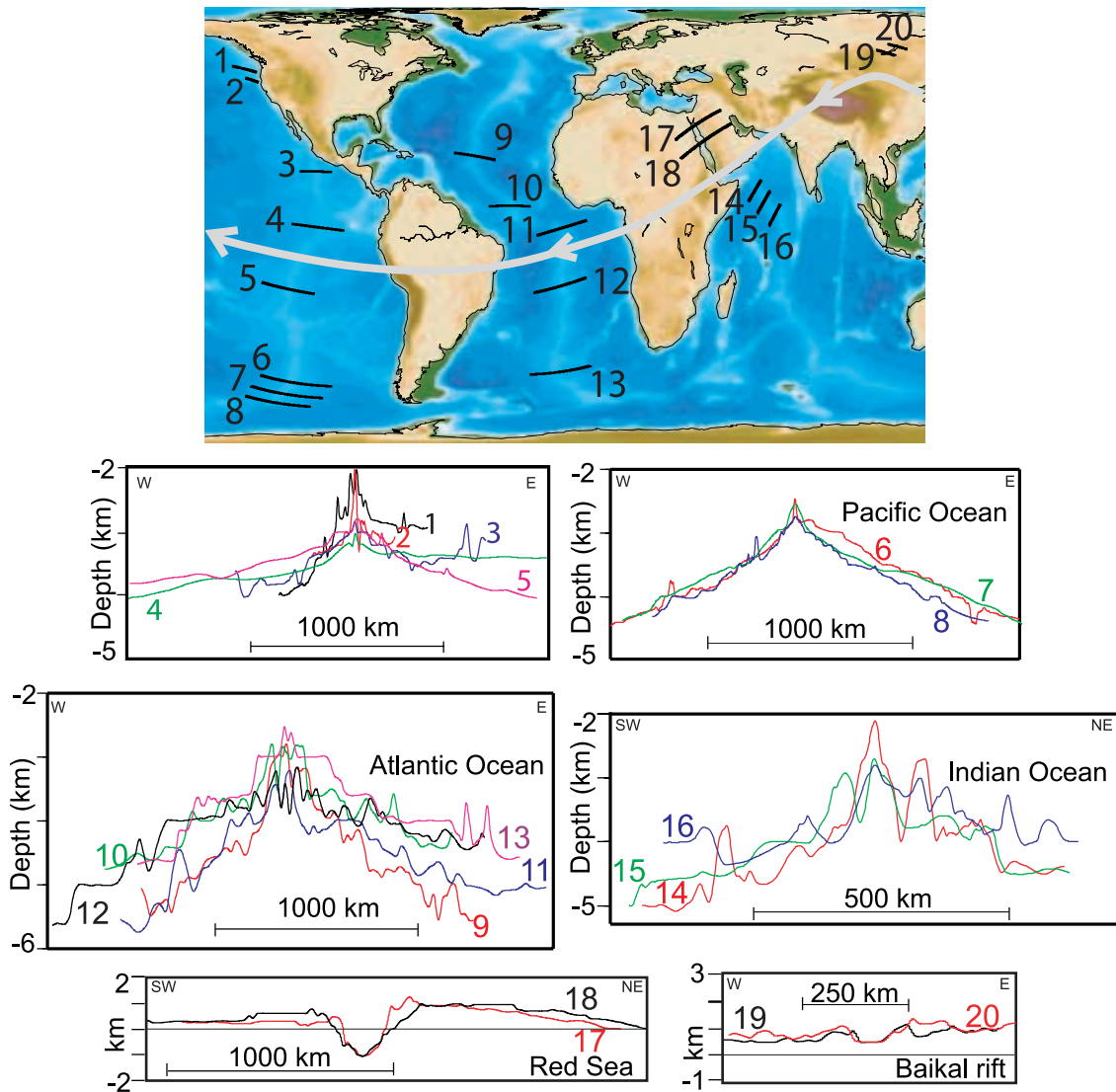
Figure 1. Topographic profiles across the major oceanic ridges and the Red Sea and Baikal rift. The locations were chosen trying to avoid seamount tracks, triple points and large deep-sea fans. Note how the eastern sides are generally more elevated. The gray sinusoidal line indicates the main direction of plate motion.

The oceanic lithosphere is differentiated mantle; therefore it is entirely controlled by mantle geochemistry, temperature and kinematics [*Anderson*, 1989]. The precise relation between mantle movements and oceanic rifts is mostly unknown, except for recent discoveries [*Silver and Holt*, 2002].

2. Asymmetric Topography Across Rift Zones

[7] In order to make representative topographic profiles of rift zones, we used the ETOPO5 data base [*National Oceanic and Atmospheric Administration* (*NOAA*), 1988], with later refinements [e.g., *Smith and Sandwell*, 1997]. We selected a number of representative sections of the most prominent rift zones (Figure 1; see Table 1 for profile coordinates). The profiles have been traced as far as possible through areas not disturbed by hot spots (which may perturb the oceanic age-depth relation [*Heestand and Crough*, 1981]), seamounts tracks, triple points, and large clastic influx of deep-sea fans. The sections are between 400 and 2200 km long, and the vertical scale is strongly amplified (e.g., $30\times$ in the Atlantic and Pacific Oceans, $12\times$ in the Indian Ocean) in order to detect elevation asymmetries not visible in physiographic maps of the ocean floors.

[8] The eastern sides of the East Pacific Rise (Figure 2), the Mid-Atlantic Ridge (MAR) (Figure 3) and the NW Indian Ridge (Figure 3) are on average more elevated than the conjugate flanks to the west or southwest as shown by topographic sections. The average larger elevation of the

Table 1. Geographic Coordinates and Length of the Topographic Profiles Shown in Figure 1

|	Western Edge		Eastern Edge		
Profile	Longitude, deg	Latitude, deg	Longitude, deg	Latitude, deg	Length, km
1	225.	46.9N	235.7	44.5N	769
2	230.	42.5N	235.	41N	431
3	250.	14.3N	262.	14.1N	1293
4	247.	0.3N	266.5	1.5S	2177
5	236.	15.3S	255.5	18.5S	2103
6	235.4	43.6S	262.	47.8S	2106
7	232.	47.7S	258.5	52.6S	1952
8	230.	51.7S	254.	56.5S	1643
9	306.6	19.4N	322.	17.4N	1639
10	319.5	5N	335.	5N	1716
11	337.	2.8S	355.5	1.2N	2104
12	336.	18.2S	355.5	14.S	2133
13	334.5	43.4S	357.	40.3S	1889
14	55.	6.2N	59.7	12N	825
15	58.2	3N	63.	9.1N	861
16	62.5	0.3S	66.8	5.6N	811
17	28.	23N	45.	32.N	1948
18	30.	17.7N	48.7	27.8N	2217
19	102.	53.5N	109.	51N	551
20	104.	54.5N	111.5	52N	570

eastern side is in the order of ~100–300 m. Opposite larger elevation to the west (e.g., section 5 in the central Pacific) or spikes deviating from the average elevation are usually associated to local seamounts (e.g., section 11 in the Atlantic, or section 14 in the Indian Ocean), due to horsts, volcanoes or extensive magmatic provinces. Bathymetry seems undistinguishable between the two flanks in the early stages of the oceanic rift (Figures 2 and 3). The shallower behavior of the eastern side becomes appreciable starting at least 50–100 km away from the ridge.

[9] In order to test this general asymmetry, the bathymetry has also been plotted versus the square root of age. Figures 4 and 5 show depth versus $age^{1/2}$ plots for the same traces shown in Figure 1. The ocean floor ages were taken from the GMT globalage_1.3.grd file, based on the work by *Müller et al.* [1997]. In the adopted version 1.3, the *Müller et al.* [1997] Pacific-Nazca isochrons were replaced with others based on new magnetic anomaly picks in French Polynesia from *Munschy et al.* [1996]. The linearization of depth-$age^{1/2}$ plots was obtained using the trend2d command of GMT software [*Wessel and Smith*, 1995]. The depth-$age^{1/2}$ plots confirm the observations done on distance versus depth plots of Figures 2 and 3. In fact, the regression lines calculated for the eastern flanks of most of the profiles (13 out of 16) are less steep with respect to regression lines calculated for the western flanks. In two sections the two slopes are almost similar (sections 6 and 8), and one is opposite (still section 5 as for bathymetry which is close to the south Pacific superswell). This indicates slower subsidence of eastern flanks, in agreement with the above outlined shallower depths. As a consequence, differences in ocean floor ages do not play a unique role in the depth asymmetry of oceans.

[10] The eastern flank of the Atlantic subsided generally more slowly than the western side [*Kane and Hayes*, 1992], probably because of density differences between the two sides, due to thermal and/or compositional differences. The MELT experiment along the East Pacific Rise [*Schreir et al.*, 1998] suggests a hotter mantle and a more elevated topography in the western side of the ridge (e.g., section 5 of Figure 1). This opposite asymmetry can be explained by the influence on the ridge of the south Pacific superswell [*McNutt and Judge*, 1990]. The same experiment also detected no deep mantle upwelling beneath the ridge, demonstrating that oceanic spreading is mainly a shallow, passive upper mantle process. This is possible if lithosphere and asthenosphere are sufficiently decoupled, as required by the westward drift of the lithosphere hypothesis. However,
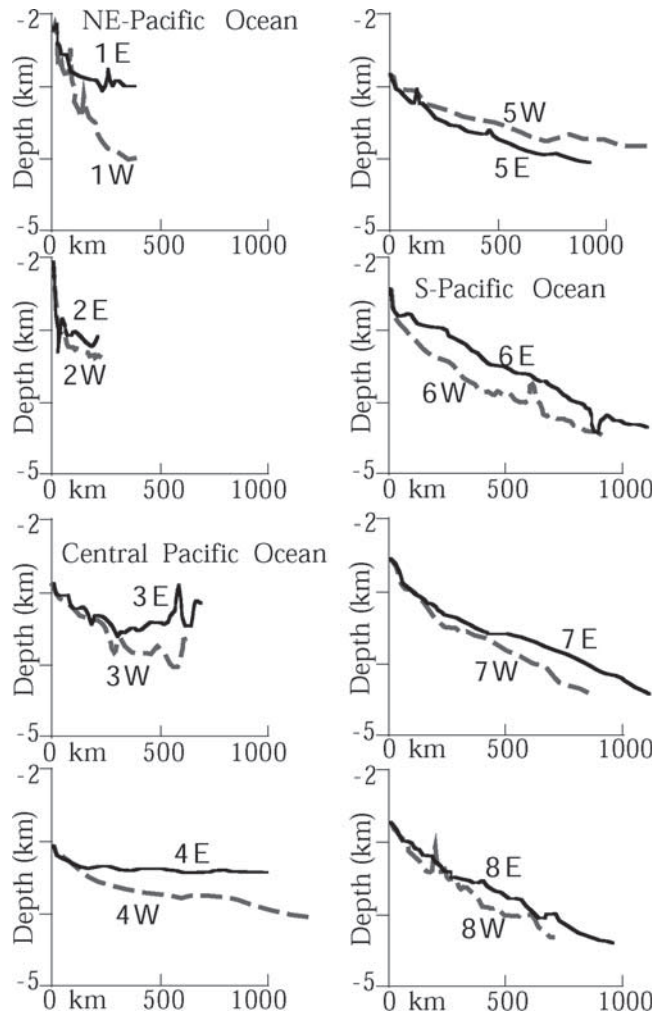
Figure 2. Topographic profiles across the Pacific Ocean. The western (W) and eastern (E) sides are plotted together in order to better appreciate the altitude differences. Gray dashed lines represent the western flanks, whereas the thick black lines are the eastern flanks. Eastern flanks are on average shallower. Location and coordinates of the profiles are given in Figure 1 and Table 1.
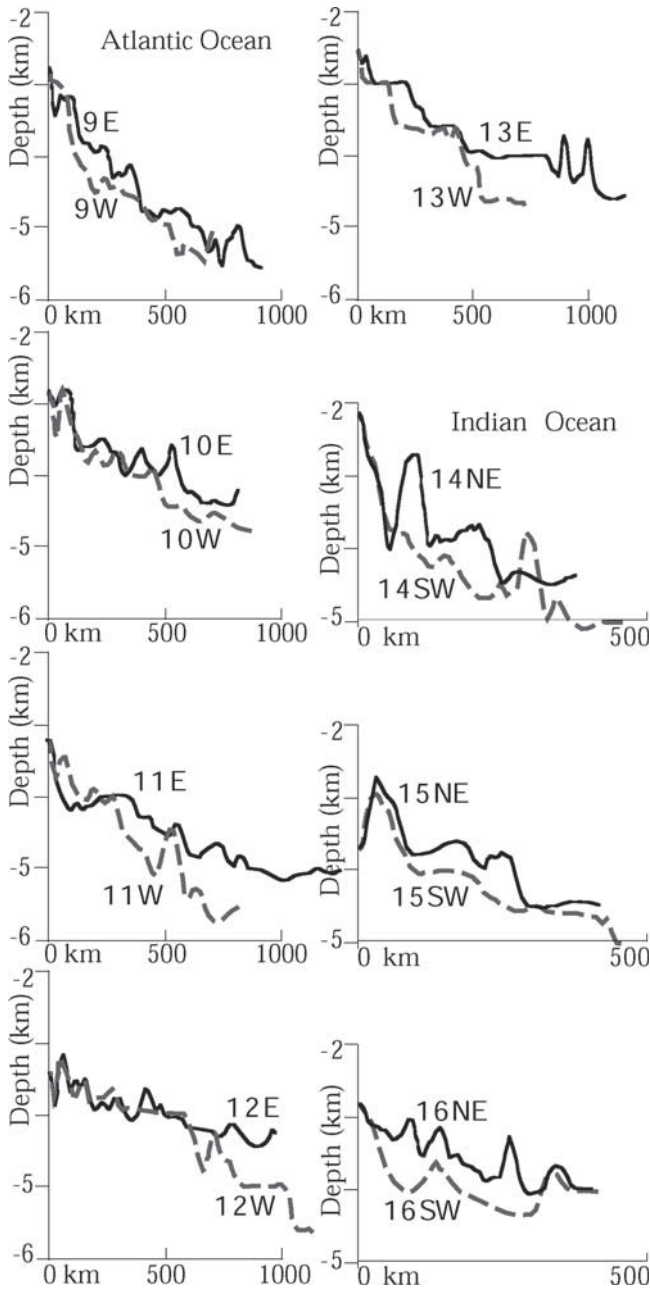
Figure 3. Topographic profiles across the Atlantic and Indian Oceans. Gray dashed lines represent the western or southwestern flanks, whereas the thick black lines are the eastern or northeastern flanks. Eastern flanks are on average shallower. Location and coordinates of the profiles are given in Figure 1 and Table 1.

passive rifting might induce secondary active upper mantle convection [*Huismans et al.*, 2001].

[11] Additional sections were made across the Red Sea and the Baikal rifts, to check whether this asymmetry occurs also along early stages of oceanic rift and continental extensional areas. The Red Sea presents a northeastern flank more elevated by ∼500 m or more, as marked also by the larger outcrop of the deep basement rocks (Figure 6).

The Baikal rift presents higher elevation of the eastern shoulder as well (Figure 6).

3. Model of Rifting

[12] A 2–4 cm yr^{-1} westward movement of the lithosphere relative to the mantle has been estimated in inde-
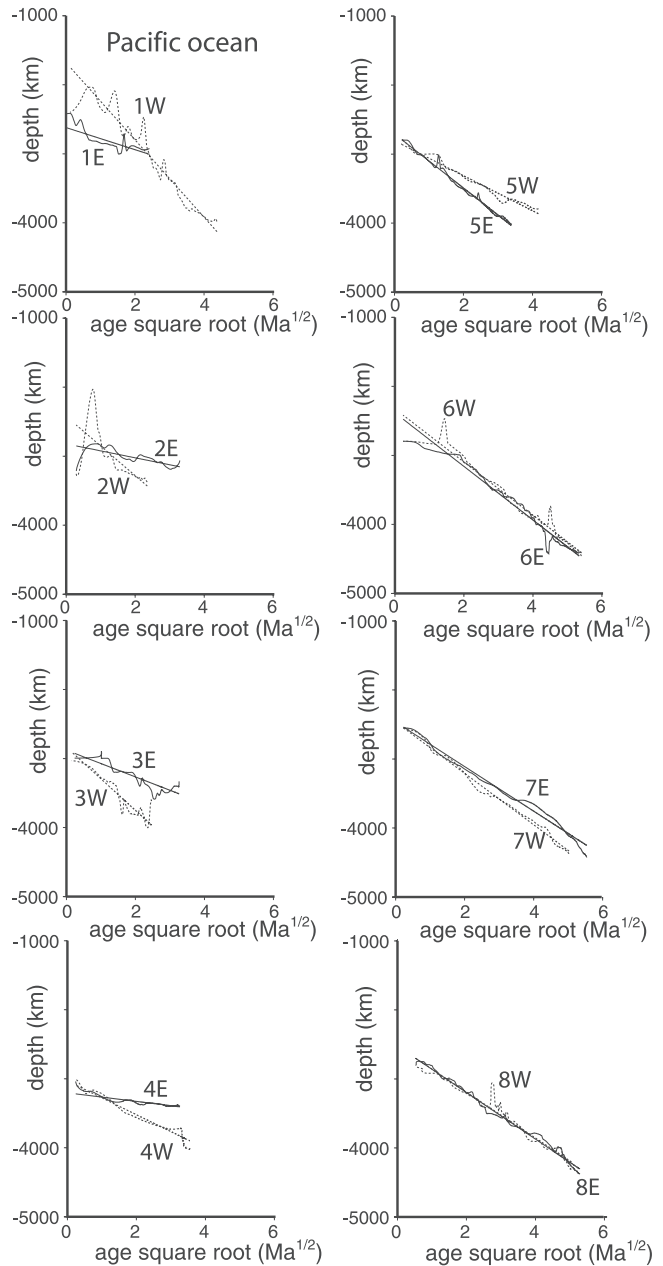

Figure 4. Elevation of the oceanic lithosphere versus square root of age in the Pacific sections. Line dots represent the western flank. The asymmetry persists showing an average less inclined mean inclination (intercept of the regression line) of the eastern flanks; the steeper slope indicates faster subsidence, which is more often in the western limb. Location and coordinates of the profiles are given in Figure 1 and Table 1.
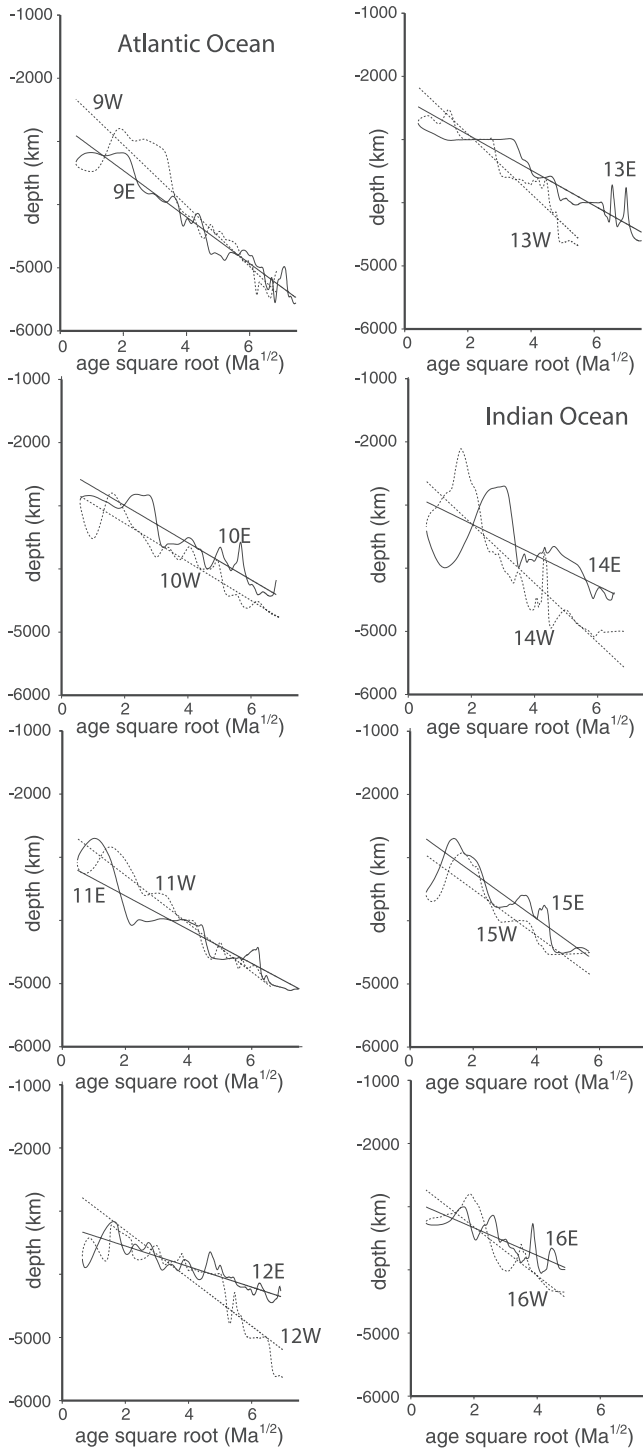
Figure 5. Elevation of the oceanic lithosphere versus square root of age in the Atlantic and Indian Ocean sections. Line dots represent the western flank. The asymmetry persists showing an average less inclined mean inclination (intercept of the regression line) of the eastern flanks; the steeper slope indicates faster subsidence, which is more often in the western limb. Location and coordinates of the profiles are given in Figure 1 and Table 1.

pendent reference frames, such as the hot spot reference frame, or geodetic and seismological data bases [*O'Connell et al.*, 1991; *Ricard et al.*, 1991; *Gordon*, 1995]. Decoupling between lithosphere and asthenosphere is considered to be variable under different plates [*Doglioni et al.*, 1999a], thus generating velocity gradients and plate tectonics. We now show with a simplified kinematic model (Figure 7) that the westward relative motion of the lithosphere can explain the topographic asymmetry outlined above. Our kinematic three-stage model assumes that, in a rift zone, the western plate moves westward faster relative to the mantle (5 cm yr^{-1}) than the eastern plate (3 cm yr^{-1}), producing a rift in between with an opening rate of 2 cm yr^{-1}. Passive mantle compensation of the removed lithosphere on top requires asthenosphere upwelling, mobilizing the entire underlying upper mantle column. These kinematics imply a westward displacement of the ridge relative to the mantle at intermediate velocity (4 cm yr^{-1}). Consequently, the mantle anomaly generated by partial melting at the ridge at the beginning of rifting (Figure 7, t$_1$) is progressively displaced eastward with respect to the ridge and should substitute the asthenospheric mantle underneath the ocean and eventually the continent to the east of the ridge at the speed of 3 cm yr^{-1} (Figure 7, t2). Mantle upwelling at the ridge determines decompression partial melting, which depletes the subridge asthenosphere of high-density phases, such as garnet. Moreover it lowers its Fe/Mg ratio, thus decreasing its density ($\Delta\rho - 60$ kg m^{-3}), relative to the undepleted mantle [*Oxburgh and Parmentier*, 1977]. The residual mantle, less dense and containing some fluids [*Scott and Stevenson*, 1989], when displaced to the east, should generate a mass deficit with respect to the western limb of the ridge, where this low-density mantle did not propagate. As a consequence, the migration of the depleted asthenosphere from west to east (e.g., below the Atlantic) should provide a significant topographic asymmetry due to lower densities in the eastern side, therefore partly counteracting the thermal subsidence in the eastern flank of the oceanic ridge (Figure 7, t3).

[13] Models of oceanic crust generation [*Bonatti et al.*, 1993] predict a fertile peridotitic mantle (>3300 kg m^{-3}) upwelling along ocean ridges. Partial melting up to a maximum of 25%, results in a Fe-depleted and less dense (by ~2%) harzburgite (3230 kg m^{-3}). Extracted basaltic melt (2800 kg m^{-3}) rises and forms the oceanic crust. Partial melting also induces a temperature decrease of the depleted asthenosphere. The density increase due to temperature decrease can be evaluated considering the relation $d\rho = -\rho\alpha_v dT$, where $\alpha_v = 3 \times 10^{-5}$ K^{-1} is the volumetric coefficient of thermal expansion, $\rho = 3230$ kg m^{-3} is the density and dT is the temperature decrease. Assuming a temperature decrease of 100 K, we obtain $d\rho$ of ~10 kg m^{-3}. Consequently, the density of the depleted asthenosphere, after correction for thermally induced volumetric contraction should have densities of ~3240 kg m^{-3}, far smaller than the density of the fertile asthenosphere. Therefore a lighter and colder asthenosphere is expected after melting below ridges.
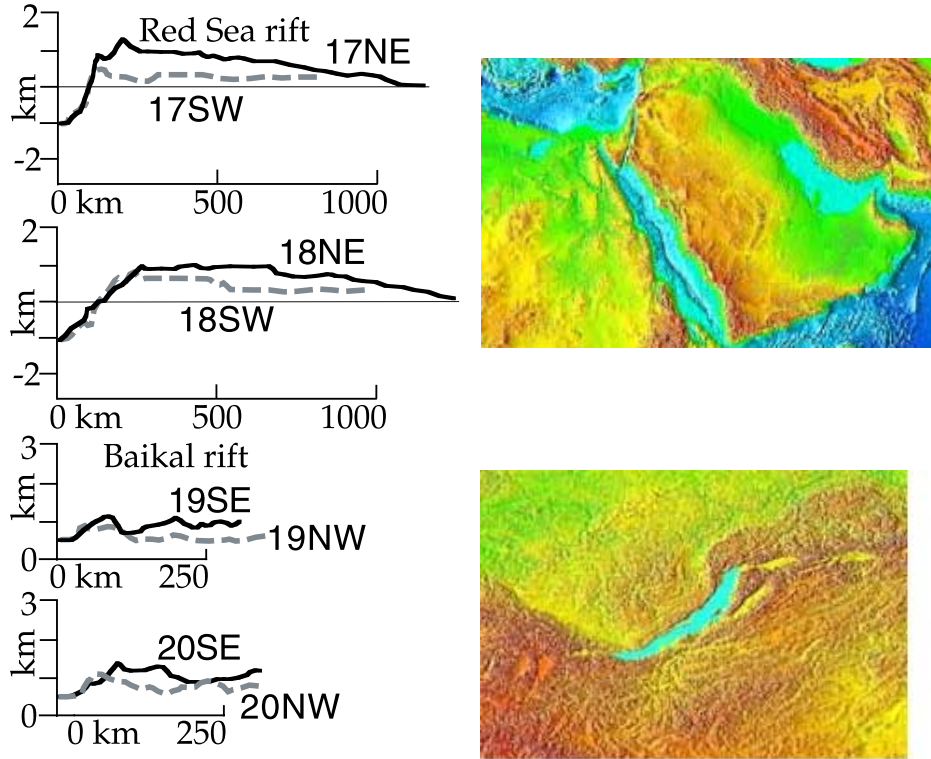
Figure 6. Topographic profiles across the Red Sea and the Baikal rift. Gray dashed lines represent the southwestern or northwestern flanks, whereas the thick black lines are the northeastern or southeastern flanks. Eastern flanks are on average shallower. Eastern flanks are on average shallower. Location and coordinates of the profiles are given in Figure 1 and Table 1.

[14] Asthenospheric uplift, a passive response to two lithospheric plates spreading apart, determines a perturbation in the upper mantle column below the ridge. The magnitude and depth extent of the density anomaly vary as a function of initial composition, water content, degree of melting, thermal gradient and mantle dynamics [*Sparks and Parmentier*, 1993; *Karato and Jung*, 1998; *Choblet and Parmentier*, 2001]. Part of the eastwardly shifted depleted asthenosphere becomes lithosphere due to cooling determining an asymmetry in the density column relative to the western flank. Moreover, when shifted eastward from the ridge, the perturbation is likely to decay partially due to cooling.

[15] Assuming isostatic equilibrium and a purely conductive heat transfer and considering the simple geometry of Figure 8a for the water-oceanic lithosphere-asthenosphere system, *Turcotte and Schubert* [1982] calculated the theoretical shape of ocean bottom. The depth of the ocean is predicted to increase with the square root of the age of the ocean floor according to

$$w = \frac{2\rho_m \alpha_v (T_m - T_0)}{\rho_m - \rho_w} \left(\frac{\kappa x}{\pi u}\right)^{1/2},$$

where ρ_m and ρ_w are the densities of asthenosphere and water, respectively; T_m and T_0 are the temperatures within

the mantle and at the surface, respectively; α_v is the volumetric coefficient of thermal expansion; κ is the mantle thermal diffusivity; x is the distance from the ridge; and u is the half spreading rate. The above simple relation predicts reasonably well the ocean deepening from the ridge crest toward the passive continental margin for ocean ages younger than 80 Ma.

[16] The model of Figure 8a is based on symmetric geometry, density and temperature distributions with respect to the ridge axis and predicts therefore equal subsidence and subsidence rates on both flanks. The kinematic model for rifting and oceanic spreading that we propose implies asymmetric settings on the two flanks of ridges. As sketched in Figure 8b, fertile asthenosphere (solid arrow) is expected to flow eastward with respect to the ridge, and asthenospheric upwelling below the ridge axis retains an eastward component of motion. At the ridge axis the upwelling asthenosphere undergoes partial melting which decreases both its density and temperature [e.g., *Fukuyama*, 1985; *Scott and Stevenson*, 1989; *Morgan*, 2001, and references therein]. After melting, the depleted (cooler and lighter) asthenosphere (dashed arrow in Figure 8b) shifts underneath the eastward flank of the ridge. For sake of simplicity, in the model of Figure 8b the asthenospheric melting is forced to occur exactly at the ridge axis. In fact, the lateral extension of melting
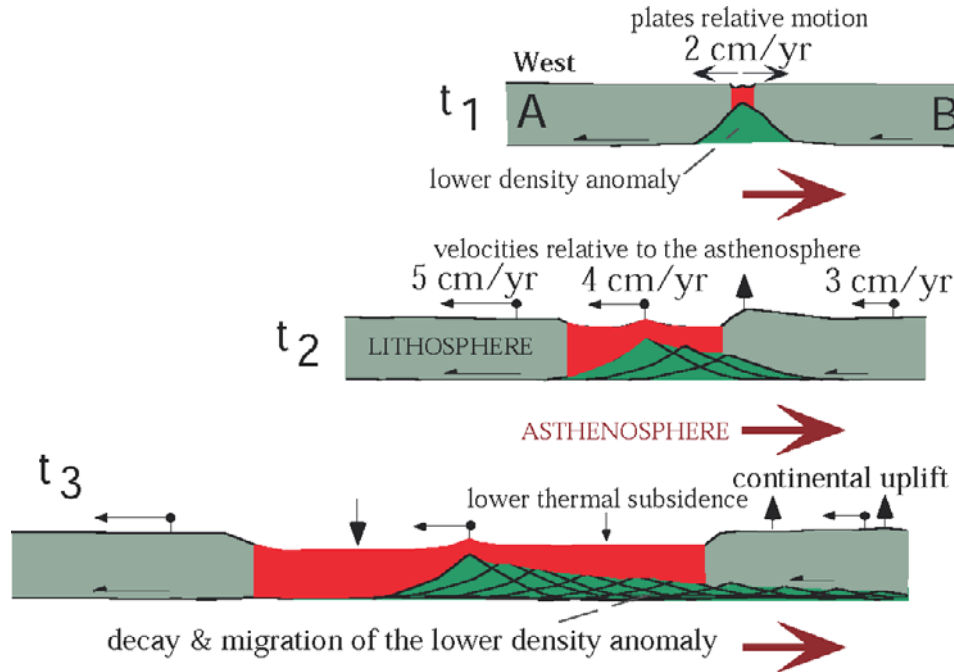
Figure 7. Kinematic three-stage model of an oceanic rift where the mantle is considered fixed and two plates A and B have variable westward velocity. Separation of the two plates determines passive upwelling and partial melting of the asthenosphere. Eastward motion of the asthenosphere relative to the lithosphere causes migration of the density anomaly, resulting in a slower subsidence in the eastern flank of the oceanic ridge and in uplift of the eastern continent.

asthenosphere at ridges spans a few tens of kilometers. This, however, does not preclude the validity of the modeling at distances greater than some 50 km from the ridge axis.

[17] Lithosphere thickening will occur at expense of undepleted and depleted asthenosphere on the western and eastern ridge flanks respectively. Since the depth at the ridge axis is the same for both flanks, the difference in mantle density and temperature underneath the two flanks will result in asymmetric bathymetry and subsidence rates. As already discussed, density increase due to partial melting of the asthenosphere could justify depleted asthenosphere density as low as 3240 kg m^{-3}. In the following calculations we assume a very conservative value of 3270 kg m^{-3} for the depleted asthenosphere density. Considering the densities and the temperatures shown in Figure 8b and assuming $\alpha_v = 3 \times 10^{-5}$ K^{-1} and $\kappa = 1$ mm^2 s^{-1} and assuming equal spreading rates on the two flanks, the above formula predicts, for any fixed floor age, shallower depths for the eastern flank (w_{east}) than for the western flank (w_{west}). The ratio between the western and eastern side depths is constant for any considered age. In particular, $w_{west}/w_{east} = 1.08$ for the parameters, densities and temperatures assumed in the calculation. For example, a w_{east} of 3000 m should correspond a w_{west} of 3227 m. Differences of some 200 m are quite common on the bathymetric profiles of Figures 2 and 3.

[18] The present-day Atlantic is a well-developed oceanic basin, conceptually similar to stage t3 of Figure 7.

The observed asymmetry of the bathymetry (Figure 3) is consistent with model predictions. In the southern Atlantic, lithospheric thickness [*Nyblade et al.*, 2000] in the western side is also larger (100–125 km) than the eastern one (75–100 km). The eastward propagating density deficit in the asthenospheric mantle could account for this asymmetry and explain mantle tomography [*Zhang and Tanimoto*, 1992; *King and Ritsema*, 2000], showing lower asthenospheric velocities in the eastern side of the Atlantic Ocean. The lower *S* wave velocities in the eastern side have been ascribed to the "hot spot" volcanism of Saint Helena, but they also persist outside this alignment.

[19] Magmatic tracks occur in both sides of the MAR. However, the distribution in the central and southern Atlantic of intense igneous activity associated with oceanic islands (Canaries, Capoverde, Saint Helena, Tristan da Cuna) and with aseismic ridges (Walvis and Rio Grande Rise) is asymmetric, being prevalent on the eastern side of the basin [*Gallagher and Hawkesworth*, 1994]. This activity is frequently ascribed to hot plumes upwelling from the deep mantle [*Morgan*, 1993]. However, at least some of these melting anomalies may have a shallow source, as suggested by their low ^{3}He/^{4}He ratios [*Kurz and Jenkins*, 1982] and other evidence [*Anderson*, 2001]. It is possible that they are caused not only by mantle thermal anomalies but also by relatively shallow mantle sources volatiles (H$_2$O)-rich that favor melting [*Bonatti*, 1990]. The presence of a shallow asthenosphere close to
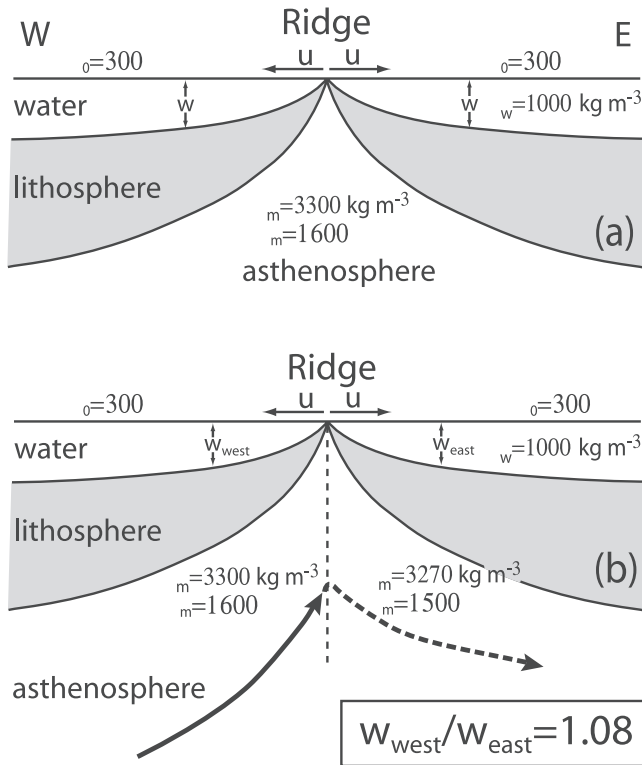
Figure 8. Geometry, density and temperature distributions adopted for the modeling of ocean bathymetry, where ρ_m and ρ_w are the densities of asthenosphere and water, respectively; T_m and T_0 are the temperatures within the mantle and at the surface, respectively; u is the half-spreading rate; and w is the water thickness. (a) The generally accepted classical symmetric scenario [e.g., *Turcotte and Schubert*, 1982]. (b) The asymmetric configuration of lithosphere formation proposed in this work. The solid arrow represents the trajectory of fertile lithosphere, moving eastward with respect to the ridge and upwelling underneath the ridge axis (dashed line). The dashed arrow represents the trajectory of depleted (lighter and colder) asthenosphere shifting eastward from the ridge. With the asymmetrical configuration (Figure 8b) the water thickness is thinner in the right side because the ratio w_{west}/w_{east} is larger than 1. For example, for a water depth of 3000 m on the eastern side, the western correspondent water section would be 3200 m deep. See text for model's details.

the melting point, and shifted from the ridge to the east, would favor stronger magmatism in the eastern side of the MAR.

4. Continental Uplift

[20] Why continents rise? Africa stands unusually high for a continent that has not undergone recent compressive tectonics, and it has a distinctive hypsometry reflecting broad-scale uplift [*Harrison et al.*, 1983]. Except for internal rift zones (e.g., the Congo Basin, the East Africa rift, etc.), Africa experienced the largest uplift of all the continents

during the Mesozoic and the Tertiary; today it stands higher than any other continent (Figure 9). A large part of Africa is above 1000 m [*Bond*, 1979]. Gravity anomalies of up to ±25 mGal and wavelength of ~2000 km correlate with regional changes in topography [*Hartley et al.*, 1996] and show a lineation of the mantle-related long-wavelength gravity field in the direction of absolute African plate motion, implying a possible SW-NE mantle flow.

[21] On the basis of the spatial distribution of Cretaceous and Tertiary sediments, *Bond* [1979] identified areas of Africa with evidence of uplift since the Late Cretaceous. These areas (Figure 10) are located in northern Africa, east of the oldest Jurassic portion of the Atlantic Ocean. Evidence for Tertiary uplift was found [*Bond*, 1979] for the areas east of the Cretaceous Atlantic opening. This broad-scale picture is confirmed by quantitative studies on vertical motions, although large areas of Africa remain unconstrained. Apatite fission track (AFT) data cover only the areas affected by Tertiary rifting (Figure 10). The upper Cretaceous uplift in northern and central Africa is supported by the following AFT data: (1) uplift stage >61 Ma in the
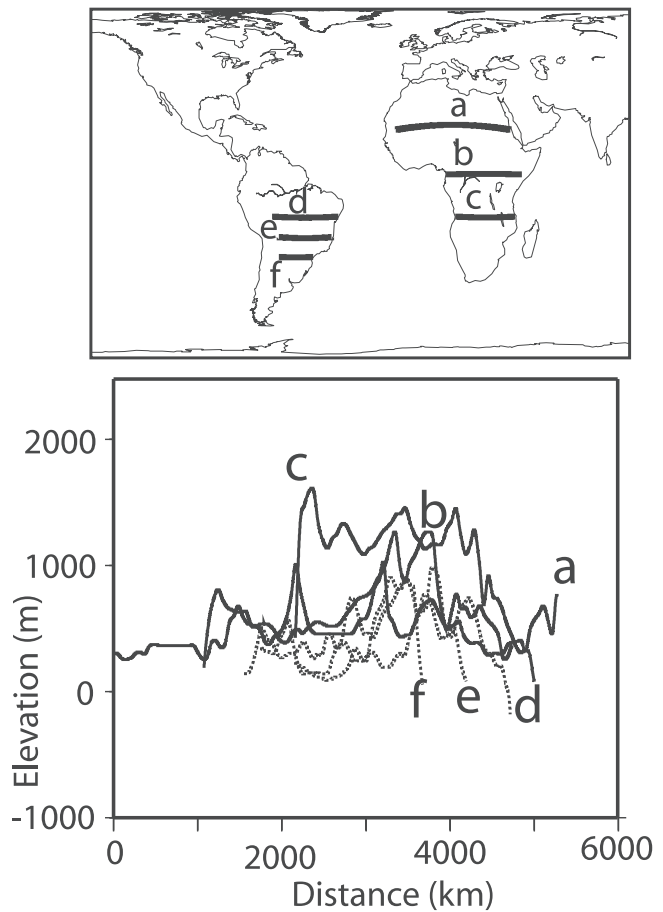
Figure 9. Comparison of representative topographic profiles of South America and Africa continents, apart the Andean orogen. South America profiles have been positioned in the most elevated areas of the continent; nevertheless, Africa has higher average elevation.
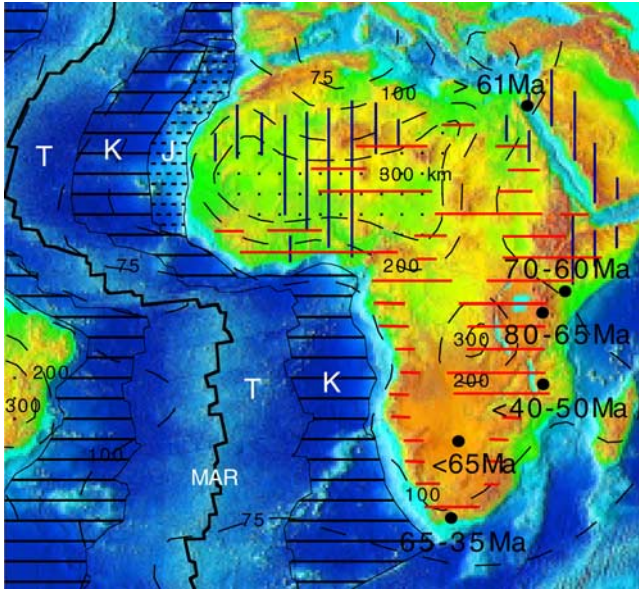
Figure 10. Areas of Africa marked by uplift since late Cretaceous (vertical blue lines) and Tertiary (horizontal red lines) after *Bond* [1979]. The earlier uplift in northern Africa follows the earlier Jurassic (J) opening of the central Atlantic. The lower topography of northern Africa corresponds to the area with thickest lithosphere (thickness values after *Pollack and Chapman* [1977]). See discussion in the text. Uplift stages from AFT data are shown. Topographic base map after NOAA.

Sinai [*Omar and Steckler*, 1995], (2) 70–60 Ma uplift in the Kenia rift flanks [*Foster and Gleadow*, 1993], and (3) 80–65 Ma uplift in the eastern Tanzania rift flanks [*Noble et al.*, 1997]. Younger uplift in southern Africa is supported by Tertiary uplift (<40–50 Ma) obtained with AFT techniques in the Malawi-Rukwa rift flanks [*Van der Beek et al.*, 1998]. Stratigraphic analysis also suggests a Tertiary (65–35 Ma) uplift stage in the Gamtoos basin, South Africa [*Thomson*, 1999], and a post-Karoo-rifting (possibly upper Tertiary) uplift in the Cabora Bassa Basin, Zimbawe [*Shoko and Gwavava*, 1999].

[22] Unlike the Pacific and Indian Ridges that have subduction zones to the east or northeast, the Atlantic Ocean shows a time correlation between spreading and subsequent uplift of the African plate to the east, suggesting some cause/effect relation between the two processes. The uplift of Africa has generally been ascribed to dynamic topography induced by mantle superplumes, i.e., mostly vertical mantle ascent [*Burke and Whiteman*, 1973; *Thiessen et al.*, 1977, 1979; *Lithgow-Bertelloni and Silver*, 1998; *Artyushkov and Hofmann*, 1998; *Gurnis et al.*, 2000, and references therein].

[23] The central North Atlantic opened between 180 and 154 Ma (Figure 10). The remaining southern portions of the Atlantic started opening later, progressively from south to north. Our model, linking oceanic rifting and continental uplift, would predict a diachronous uplift between northern and southern Africa, from Jurassic to recent times.

[24] The kinematics proposed in the previous section should generate a significant uplift wave able to transit below the continent to the east or northeast of the ridge. According to model velocities, the depleted asthenosphere would move 3000 km to the east in 100 Ma. Progressive opening causes the distance between the ridge and the continents to increase. The low-velocity zone is in general very thin under shields, extending from ~150 to 200 km, whereas it goes from a few km depths, down to 400 km underneath some oceanic ridges [*Anderson*, 1989]. A maximum lithospheric thickness of ~250 km has been detected under Africa (West African, Congo, Kalahari and Tanzania cratons [*Ritsema and van Heijst*, 2000; *Nyblade et al.*, 2000]). A global reference of lithospheric thickness has been proposed by *Pollack and Chapman* [1977], a map with sufficient resolution considering the scale of the present study. *Pollack and Chapman* [1977] show an average thickness of ~75 km in the Atlantic, with maximum thickness in the southwestern side (100 km). Moving from the oceanic ridge to the continent, the upper and lower boundaries of the asthenosphere tend to converge. The upper asthenosphere boundary along the MAR dips toward Africa at an average low angle of ~1°, whereas it increases to ~3° from the continental margin to the deepest shield. The lower asthenosphere boundary, moving from the MAR to the continental root probably rises at an average angle of 1°. Thinning of the asthenospheric channel below continents should cause faster flow of the mantle due to the Bernoulli Principle.

[25] We attempted some modeling, under the assumption that a density anomaly of -20 kg m^{-3} still affects the anomalous asthenosphere column when shifted underneath the continent. We also assume local isostasy and consider a column composed by a 40 km thick continental crust (density of 2800 kg m^{-3}), a lithospheric mantle (LID) of 60 km (3370 kg m^{-3}) and by 50 km (a part of) of asthenosphere (3400 kg m^{-3}, Figure 11). Density values are consistent with the PREM [*Anderson*, 1989], which suggests average density up to 2900 kg m^{-3} in the crust and 3370 kg m^{-3} in the LID, whereas the asthenosphere may have density as low as 3350 kg m^{-3}. An upper mantle with relative lower density under the Colorado plateau has been considered the reason for the Cenozoic uplift of that continental area [*Parsons and McCarthy*, 1995].

[26] Assuming an arbitrary compensation depth within the asthenosphere at 150 km, we would expect a load of ~4842 MPa. The replacement of the original (3400 kg m^{-3}) with lighter asthenosphere (3380 kg m^{-3}) would produce an uplift of ~330 m, necessary in order to keep constant the load at the assumed compensation depth. Increasing the thickness of the asthenosphere down to 200 km and assuming a 200 km compensation depth, would double to 660 m the isostatic continental rebound (Figure 11).

[27] Keeping fixed the compensation depth, larger lithospheric thicknesses decrease the asthenosphere section and therefore produce lower isostatic uplift. Note that central southern Africa (where lithospheric thickness is lower) underwent post-Atlantic rift uplift larger than thicker northern Africa (Figure 10). This would explain the paradox of
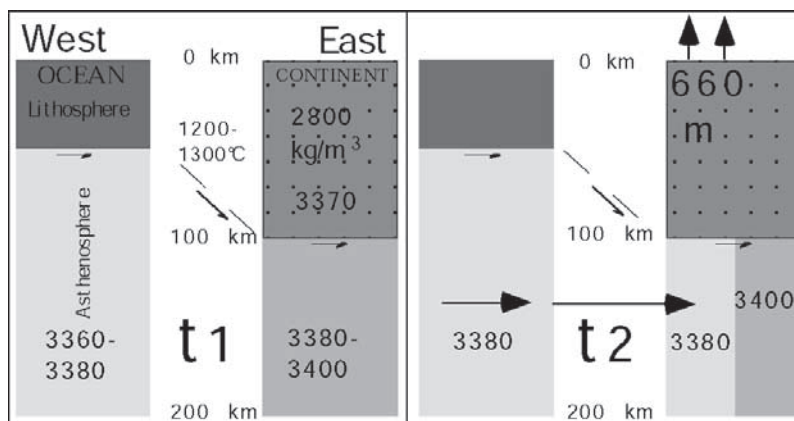
Figure 11. Low-density asthenosphere replaces "normal" asthenosphere below a continent (stage t2), thereby causing uplift.

higher topography where the continental lithosphere is thinner, as in southern Africa.

[28] Uplift should be maximal as the low-density anomaly flows beneath the continent; subsequently, in a steady state transit, it should stabilize or decrease. Africa is more uplifted in the central southern part, east of the Cretaceous Atlantic Ocean, whereas the northern part of the continent, with a lower topography (Figure 10), is located eastward of the oldest Jurassic part of the Atlantic. The West Africa continental margin acts as an active hinge zone between the uplifting continent and the subsiding ocean.

[29] A significant morphologic high occurs also in central southern India, and its origin could be similar to that for Africa, but related to the opening of the Indian Ocean. South America is located eastward of the Pacific ridges, but the intervening Andean subduction is probably limiting the passage of the depleted asthenosphere. Topographic comparison between Africa and South America, excluding the Andean orogen, confirms the higher average topography in the continent eastward of the Atlantic Ocean (Figure 9).

[30] The Red Sea rift provides another test for the model, similar to the early stages of Figure 6. A striking elevation asymmetry can be observed on the two flanks of the rift zone, the eastern flank showing far higher elevations than the western one. The uplift mainly occurred during the Pliocene and Quaternary. The Gulf of Suez, Red Sea and Gulf of Aden opening and their asymmetry have been interpreted in a number of ways (e.g., the plate size where the larger uplift of Sinai and Arabia with respect to Africa is due to their smaller size; asthenospheric advection; initiation of other concomitant geodynamic processes such as the Aqaba rift [*Moretti and Chénet*, 1987; *Colletta et al.*, 1988; *Patton et al.*, 1994; *Ghebreab*, 1998, and references therein]). In the Red Sea-Suez Gulf, the uplift of the shoulders occurred after the initiation of the rift [*Garfunkel and Bartov*, 1977; *Moretti and Chénet*, 1987]. Moreover, the rapid subsidence in the rift and uplift of the shoulders cannot be due to purely thermal processes [*Moretti and Chénet*, 1987]). Therefore the Red Sea and Gulf of Suez

support a model of initial stretching of the lithosphere, contemporaneous asthenospheric uplift and subsidence in the rift itself for the upraise of the underlying high-density mantle rocks. In the meanwhile, the lateral shift of the depleted mantle below unstretched continental lithosphere and substitution of undepleted asthenosphere could explain the larger uplift of the northeastern shoulder. Low Q values are also indicated below the Arabia plate [*Mitchell et al.*, 1997].

[31] Most of the proposed models in this area as elsewhere do not consider the decoupling between lithosphere and underlying mantle. As an alternative hypothesis, we suggest that the relative eastward or northeastward mantle flow could explain the differences between the two continental margins. The Baikal rift [*Ionov*, 2002] shows asymmetric topography, which could be interpreted in a similar way. The Red Sea and the Baikal rift are almost perpendicular to each other. In fact the higher rift flank elevation is located respectively to the northeast and to the southeast. However, the rifts are located at right angle relative to the global flow of plates motion (Figure 1), which is sinusoidal, and not simply E-W [*Doglioni et al.*, 1999a]. Strictly along the axis of the two rifts, the topography does not show significant asymmetry. This would suggest that asymmetry becomes significant only at mature stages of oceanization, but it is more rapidly recorded under the continental lithosphere to the east.

5. Westward Drift of the Lithosphere and Discussion

[32] Mantle anisotropy provides evidence of mantle flow, e.g., beneath western North America [*Silver and Holt*, 2002] and beneath the southern Pacific rise [*Wolfe and Solomon*, 1998]. *Kennedy et al.* [2002] have shown how mantle xenoliths recorded a shear possibly located at the lithosphere-asthenosphere interface. This supports the notion of a flow in the upper mantle and some decoupling at the base of the lithosphere [*Russo and Silver*, 1996; *Doglioni et al.*,

1999a; *Bokelman and Silver*, 2000]. However, we still do not know how plates and the entire lithosphere move relative to the mantle.

[33] There are two reference frames for measuring plate motion: the no-net-rotation (NNR) reference frame and the hot spot reference frame. The first has been constructed in two ways, either on the base of seismicity and magnetic anomalies [*DeMets et al.*, 1990], or, in the last decade, on the base of space geodesy [e.g., *Robbins et al.*, 1993]. The hot spot reference frame is based on plate motion relative to hypothetically fixed deep mantle sources rotation [*Gripp and Gordon*, 1990; *Argus and Gordon*, 1991; *Ricard et al.*, 1991]. The NNR reference frame is anchored to a hypothetic fixed Earth's center and does not tell us what the lithosphere is doing relative to the underlying mantle.

[34] Assuming the hot spot reference frame, the velocity of the Pacific plate toward west-northwest is so high that summing all vectors oriented in other directions, a residual component of mean lithosphere motion toward the west is observed, in the sense of nonzero toroidal field of degree one [*Ricard et al.*, 1991]. In other words, the lithosphere has a net westward rotation, but this rotation is at present a kinematic parameter, not necessarily a physical rotation of the entire outer shell with respect to the deep lower mantle. Another way of saying this is that the mean lithosphere velocity involves a westward motion of the entire lithosphere system with respect to the deep lower mantle. If one adds up the cross product of the velocity with the radial vector over the entire surface of the Earth, then there is a net rotation that is nonzero in the hot spot frame.

[35] The key point is to consider what individual plate-ridge-plate systems are doing in the hot spot frame itself, not only what the mean lithosphere motion is doing. If one examines Africa–South America in the hot spot frame, Africa is barely moving or it would move northeastward relative to the mantle [e.g., *Müller et al.*, 1993]. Thus Africa would never override the more buoyant residual ridge mantle material as proposed here, unless it has a westward motion with respect to the lower mantle.

[36] Nevertheless, growing evidence suggests that the so-called hot spots, on which the "absolute" motion of Africa has been computed, are rather superficial features, originating either from the asthenosphere or the lithosphere itself [*Bonatti*, 1990; *Smith*, 1993; *Anderson*, 1999, 2000, 2001; *Smith and Lewis*, 1999; *Harpp et al.*, 2002]. Thus the widespread African magmatism [*Morgan*, 1972; *Burke et al.*, 1973; *Burke and Wilson*, 1976; *Morgan*, 1983] might be unrelated to deep mantle sources, and therefore not be a suitable reference frame for plate motion. African magmatism could be rather triggered by the passage of the underlying lighter asthenosphere.

[37] Moreover, oceanic ridges are moving one respect to the other (e.g., Atlantic and Indian Ridges are moving away from Africa), increasing the distance between the two rifts and suggesting that the lithosphere is decoupled from the underlying mantle [*White and McKenzie*, 1995]. Therefore

hot spots which are persistently located along oceanic ridges (Azores, Ascencion, Tristan da Cuna, Galapagos) cannot be considered fixed [e.g., *Burke et al.*, 1973]. Moreover the northeastward motion of Africa detected by space geodesy is relative to a NNR reference frame, unrelated to what the mantle is doing. The absence of the westward drift as an entire lithospheric delay (and not only of a few plates) relies on the now weaker evidence of the deep source and fixity of hot spots.

[38] As for subduction zones asymmetry, the westward drift can be inferred also by geological and geophysical asymmetries along rift zones, independently of the obsolete hot spot reference frame. Therefore the mantle could move northeastward underneath Africa faster than the lithosphere. This would be possible if the African lithosphere were sufficiently decoupled from the mantle, which is easier if below Africa there is a lower lithosphere or upper asthenosphere containing some melt sourcing its so-called hot spots along rift zones. Evidence for eastward mantle flow is the eastward retreat of the west directed Apennines subduction zone, which occurs along the northern prolongation of Africa, i.e., the Adriatic plate or African promontory. Whether it is the cause or the consequence, the slab retreat requires eastward mantle motion both in the hanging wall and in the footwall of the slab [*Doglioni et al.*, 1999b].

6. Conclusions

[39] Although not predicted by classic plate tectonics theory, the eastern sides of most of the Earth's rift zones have an average higher elevation of 100–300 m. This affects not only the oceanic lithosphere, but also the continents to the "east", e.g., Africa and Arabia, several hundreds or thousands km away from the rift. The asymmetry could be explained by a shift to the east of the asthenosphere previously depleted along the rift zone, and producing a mass deficit relative to the western counterpart. Therefore continental uplift can be accounted for not only by vertical mantle motion, but also by horizontal substitution of undepleted denser mantle with a slightly depleted mantle that causes upward isostatic readjustment. The eastward motion of the mantle in the oceans and beneath Africa would be a further support to a globally persistent relative westward drift of the lithosphere along the sinusoidal flow lines of plate motion [*Doglioni et al.*, 1999a], reconciling the geological and geophysical asymmetries observed both along subduction and rift zones. The so-called hot spots are a misleading reference frame for measuring plate motion relative to the mantle, because they are not fixed and they might partly originate in the lower lithosphere or the asthenosphere [*Anderson*, 1999; *Smith and Lewis*, 1999].

References

Anderson, D. L., *Theory of the Earth*, 366 pp., Blackwell, Malden, Mass., 1989.

Anderson, D. L., A theory of the Earth: Hutton and Humpty-Dumpty and Holmes, in *James Hutton: Present and Future*, edited by G. Y. Craig and J. H. Hull, *Geol. Soc. Spec. Publ.*, *150*, 13–35, 1999.

Anderson, D. L., Thermal state of the upper mantle: No role for mantle plumes, *Geophys. Res. Lett.*, *27*, 3623–3626, 2000.

Anderson, D. L., A statistical test of the two reservoir model for helium, *Earth Planet. Sci. Lett.*, *193*, 77–82, 2001.

Argus, D. F., and R. G. Gordon, No-net-rotation model of current plate velocities incorporating plate motion model NUVEL-1, *Geophys. Res. Lett.*, *18*, 2039–2042, 1991.

Artyushkov, E. V., and A. W. Hofmann, Neotectonic crustal uplift on the continents and its possible mechanisms; the case of southern Africa, *Surv. Geophys.*, *19*, 369–415, 1998.

Bokelman, G. H., and P. G. Silver, Mantle variation within the Canadian Shield: Travel times from the portable broadband Archean-Proterozoic transect 1989, *J. Geophys. Res.*, *105*, 579–605, 2000.

Bonatti, E., Not so hot "hot spots" in the oceanic mantle, *Science*, *250*, 107–111, 1990.

Bonatti, E., M. Seyler, and N. Sushevskaya, A cold suboceanic mantle belt at the Earth's equator, *Science*, *261*, 315–320, 1993.

Bond, G. C., Evidence for some uplifts of large magnitude in continental platforms, *Tectonophysics*, *61*, 285–305, 1979.

Bostrom, R. C., Westward displacement of the lithosphere, *Nature*, *234*, 356–538, 1971.

Burke, K., and A. J. Whiteman, Uplift, rifting and the break-up of Africa, in *Implications of Continental Drift to the Earth Sciences*, vol. 2, part 7, *Rifts and Oceans*, edited by D. H. Tarling and S. K. Runcorn, pp. 735–755, Academic, San Diego, Calif., 1973.

Burke, K., and J. T. Wilson, Hotspots on the Earth's surface, *Sci. Am.*, *235*(2), 46–57, 1976.

Burke, K., W. S. F. Kidd, and J. T. Wilson, Relative and latitudinal motion of Atlantic hotspots, *Nature*, *245*, 133–137, 1973.

Calcagno, P., and A. Cazenave, Subsidence of the seafloor in the Atlantic and Pacific oceans; regional and large-scale variations, *Earth Planet. Sci. Lett.*, *126*, 473–492, 1994.

Carlson, R. L., and S. T. Johnson, On modeling the thermal evolution of the oceanic upper mantle: An assessment of the cooling plate model, *J. Geophys. Res.*, *99*, 3201–3214, 1994.

Choblet, G., and E. M. Parmentier, Mantle upwelling and melting beneath slow spreading centers: Effects of variable rheology and melt productivity, *Earth Planet. Sci. Lett.*, *184*, 589–604, 2001.

Colletta, B., P. Le Quellec, J. Letouzey, and I. Moretti, Longitudinal evolution of the Suez rift structure (Egypt), *Tectonophysics*, *153*, 221–233, 1988.

DeMets, C., R. G. Gordon, D. F. Argus, and S. Stein, Current plate motions, *Geophys. J. Int.*, *101*, 425–478, 1990.

Doglioni, C., P. Harabaglia, S. Merlini, F. Mongelli, A. Peccerillo, and C. Piromallo, Orogens and slabs vs their direction of subduction, *Earth Science Reviews*, *45*, 167–208, 1999a.

Doglioni, C., E. Gueguen, P. Harabaglia, and F. Mongelli, On the origin of W-directed subduction zones and applications to the western Mediterranean, in *The Mediterranean Basins: Tertiary Extensions Within the Alpine Orogen*, edited by B. Durand et al., *Geol. Soc. Spec. Publ.*, *156*, 541–561, 1999b.

Foster, D. A., and A. J. W. Gleadow, Episodic denudation in East Africa: A legacy of intracontinental tectonism, *Geophys. Res. Lett.*, *20*, 2395–2398, 1993.

Fukuyama, H., Heat of fusion of basaltic magma, *Earth Planet. Sci. Lett.*, *73*, 407–414, 1985.

Gallagher, K., and C. Hawkesworth, Mantle plumes, continental magmatism and asymmetry in the South Atlantic, *Earth Planet. Sci. Lett.*, *123*, 105–117, 1994.

Garfunkel, Z., and Y. Bartov, The tectonics of the Suez rift, *Geol. Surv. Isr.*, *71*, 1–41, 1977.

Ghebreab, W., Tectonics of the Red Sea region reassessed, *Earth Sci. Rev.*, *45*, 1–44, 1998.

Gordon, R. G., Present plate motions and plate boundaries, in *Global Earth Physics*, *AGU Ref. Shelf*, vol. 1, edited by T. J. Arhens, pp. 66–87, AGU, Washington, D. C., 1995.

Gripp, A. E., and R. G. Gordon, Current plate velocities relative to the hotspots incorporating the NUVEL-1 global plate motion model, *Geophys. Res. Lett.*, *17*, 1109–1112, 1990.

Gurnis, M., J. Mitrovica, J. Ritsema, and H. J. van Heijst, Constraining mantle density structure using geological evidence of surface uplift rates: the case of the African superplume, *Geochem. Geophys. Geosyst.*, *1*, Paper number 1999GC000035, 2000.

Harabaglia, P., and C. Doglioni, Topography and gravity across subduction zones, *Geophys. Res. Lett.*, *25*, 703–706, 1998.

Harpp, K. S., K. R. Wirth, and D. J. Korich, Northern Galapagos Province: Hotspot-induced, near ridge volcanism at Genovesa Island, *Geology*, *30*, 399–402, 2002.

Harrison, C. G. A., K. J. Miskell, G. W. Brass, E. S. Saltzman, and L. Sloan, Continental hypsography, *Tectonics*, *2*, 357–377, 1983.

Hartley, R., A. B. Watts, and J. D. Fairhead, Isostasy of Africa, *Earth Planet. Sci. Lett.*, *137*, 1–18, 1996.

Hayes, D. E., Age-depth relationships and depth anomalies in the southeast Indian Ocean and South Atlantic Ocean, *J. Geophys. Res.*, *93*, 2937–2954, 1988.

Heestand, R. L., and S. T. Crough, The effect of hot spots on the oceanic age-depth relation, *J. Geophys. Res.*, *86*, 6107–6114, 1981.

Huismans, R. S., Y. Podladchikov, and S. Cloetingh, Transition from passive to active rifting: Relative importance of asthenospheric doming and passive extension of the lithosphere, *J. Geophys. Res.*, *106*, 11,271–11,291, 2001.

Humler, H., C. Langmuir, and V. Daux, Depth versus age: New perspectives from the chemical compositions of ancient crust, *Earth Planet. Sci. Lett.*, *173*, 7–23, 1999.

Ionov, D., Mantle structure and rifting processes in the Baikal-Mongolia region: Geophysical data and evidence from xenoliths in volcanic rocks, *Tectonophysics*, *351*, 41–60, 2002.

Jarvis, G. T., and W. R. Peltier, Oceanic bathymetry profiles flattened by radiogenic heating in convective mantle, *Nature*, *285*, 649–651, 1980.

Kane, K. A., and D. E. Hayes, Tectonic corridors in the South Atlantic: Evidence for long-lived mid-ocean ridge segmentation, *J. Geophys. Res.*, *97*, 17,317–17,330, 1992.

Karato, S.-I., and H. Jung, Water, partial melting and the origin of the seismic low velocity and high attenuation zone in the upper mantle, *Earth Planet. Sci. Lett.*, *157*, 193–207, 1998.

Kennedy, L. A., J. K. Russell, and M. G. Kopylova, Mantle shear zones revisited: The connection between the cratons and mantle dynamics, *Geology*, *30*, 419–422, 2002.

King, S. D., and J. Ritsema, Africa hot spot volcanism: Small-scale convection in the upper mantle beneath cratons, *Science*, *290*, 1137–1140, 2000.

Klein, E. M., and C. H. Langmuir, Global correlations of ocean ridge basalt chemistry with axial depth and crustal thickness, *J. Geophys. Res.*, *92*, 8089–8115, 1987.

Kurz, M. D., and W. J. Jenkins, Helium isotopic systematics of oceanic islands and mantle heterogeneity, *Nature*, *297*, 43–47, 1982.

Lithgow-Bertelloni, C., and P. G. Silver, Dynamic topography, plate driving forces and the African superswell, *Nature*, *395*, 269–272, 1998.

Marks, K. M., and J. M. Stock, Variations in ridge morphology and depth-age relationships on the Pacific-Antarctic ridge, *J. Geophys. Res.*, *99*, 531–541, 1994.

Marty, J. C., and A. Cazenave, Regional variations in subsidence rate of oceanic plates; a global analysis, *Earth Planet. Sci. Lett.*, *94*, 301–315, 1989.

McNutt, M. K., and A. V. Judge, The superswell and mantle dynamics beneath the South Pacific, *Science*, *248*, 969–975, 1990.

Mitchell, B. J., Y. Pan, X. J. Kang, and L. Cong, *Lg* coda *Q* variation across Eurasia and its relation to crustal evolution, *J. Geophys. Res.*, *102*, 22,767–22,779, 1997.

Moretti, I., and P. Y. Chénet, The evolution of the Suez Rift: A combination of stretching and secondary convection, *Tectonophysics*, *133*, 229–234, 1987.

Morgan, J. P., Thermodynamics of pressure release melting of a veined plum pudding mantle, *Geochem. Geophys. Geosyst.*, *2*, Paper number 2000GC000049, 2001.

Morgan, W. J., Deep mantle convection plumes and plate motions, *Assoc. Am. Pet. Geol. Bull.*, *56*, 203–213, 1972.

Morgan, W. J., Hotspot tracks and the early rifting of the Atlantic, *Tectonophysics*, *94*, 123–139, 1983.

Müller, R. D., J. Y. Royer, and A. L. Lawrence, Revised plate motions relative to the hotspots from combined Atlantic and Indian Ocean hotspot tracks, *Geology*, *21*, 275–278, 1993.

Müller, R. D., W. R. Roest, J. Y. Royer, L. M. Gahagan, and J. G. Sclater, Digital isochrons of the world's ocean floor, *J. Geophys. Res.*, *102*, 3211–3214, 1997.

Munschy, M., C. Antoine, and A. Gachon, Evolution tectonique de la region des Tuamotu, ocean Pacifique Central, *C. R. Acad. Sci., Ser. IIa*, *323*, 941–948, 1996.

National Oceanic and Atmospheric Administration (NOAA), ETOPO5 bathymetry/topography Data Announcement 88-MGG-02, Digital relief of the surface of the Earth, Natl. Geophys. Data Cent., U.S. Dep. of Commer., Boulder, Colo., 1988. (Available at http://www.ngdc.noaa.gov/mgg/global/seltopo.html)

Noble, W. P., D. A. Foster, and A. J. W. Gleadow, The post-Pan-African thermal and extensional history of crystalline basement rocks in eastern Tanzania, *Tectonophysics*, *275*, 331–350, 1997.

Nyblade, A. A., J. O. Thomas, H. Gurrola, J. Ritsema, and C. A. Langston, Seismic evidence for a deep upper mantle thermal anomaly beneath East Africa, *Geology*, *28*, 599–602, 2000.

O'Connell, R., C. G. Gable, and B. Hager, Toroidal-poloidal partitioning of lithospheric plate motions, in *Glacial Isostasy, Sea-Level and Mantle Rheology*, edited by R. Sabadini et al., pp. 334, 535–551, Kluwer Acad., Norwell, Mass., 1991.

Omar, G. I., and M. S. Steckler, Fission track evidence on the initial rifting of the Red Sea: Two pulses, no propagation, *Science*, *270*, 1341–1344, 1995.

Oxburgh, E. R., and E. M. Parmentier, Compositional and density stratification in oceanic lithosphere: Causes and consequences, *J. Geol. Soc. London*, *133*, 343–355, 1977.

Parsons, B., and J. G. Sclater, An analysis of the variation of ocean floor bathymetry and heat flow with age, *J. Geophys. Res.*, *82*, 803–827, 1977.

Parsons, T., and J. McCarthy, The active southwest margin of the Colorado Plateau: Uplift of mantle origin, *Geol. Soc. Am. Bull.*, *107*, 139–147, 1995.

Patton, T. L., A. R. Moustafa, R. A. Nelson, and A. S. Abdine, Tectonic evolution and structural setting of the Suez Rift, in *Interior Rift Basins*, edited by S. M. Landon, *AAPG Mem.*, *59*, 9–55, 1994.

Perrot, K., J. Francheteau, M. Maia, and C. Tisseau, Spatial and temporal variations of subsidence of the East Pacific Rise (0–23°S), *Earth Planet. Sci. Lett.*, *160*, 593–607, 1998.

Phipps Morgan, J., and W. H. F. Smith, Flattening of the seafloor depth-age curve as a response to asthenospheric flow, *Nature*, *359*, 524–527, 1992.

Pollack, H. N., and D. S. Chapman, On the regional variation of heat flow, geotherms, and lithospheric thickness, *Tectonophysics*, *38*, 279–296, 1977.

Ricard, Y., C. Doglioni, and R. Sabadini, Differential rotation between lithosphere and mantle: A consequence of lateral viscosity variations, *J. Geophys. Res.*, *96*, 8407–8415, 1991.

Ritsema, J., and H. van Heijst, New seismic model of the upper mantle beneath Africa, *Geology*, *28*, 63–66, 2000.

Robbins, J. W., D. E. Smith, and C. Ma, Horizontal crustal deformation and large scale plate motions inferred from space geodetic techniques, in *Contributions of Space Geodesy to Geodynamics-Crustal Dynamics*, *Geodyn. Ser.*, vol. 23, edited by D. E. Smith and D. L. Turcotte, pp. 21–36, AGU, Washington, D. C., 1993.

Russo, R. M., and P. G. Silver, Cordillera formation, mantle dynamics, and the Wilson cycle, *Geology*, *24*, 511–514, 1996.

Schreir, D. S., D. W. Forsyth, M. H. Cormier, and K. C. Macdonald, Shipboard geophysical indications of asymmetry and melt production beneath the East Pacific Rise near the MELT experiment, *Science*, *280*, 1221–1224, 1998.

Scott, D. R., and D. J. Stevenson, A self-consistent model of melting, magma migration and buoyancy-driven circulation beneath mid-ocean ridges, *J. Geophys. Res.*, *94*, 2973–2988, 1989.

Shoko, D. S. M., and O. Gwavava, Is magmatic underplating the cause of post-rift uplift and erosion within the Cabora Bassa Basin, Zambesi rift, Zimbawe?, *J. Afr. Geol.*, *28*, 465–485, 1999.

Silver, P. G., and W. E. Holt, The mantle flow field beneath western North America, *Science*, *295*, 1054–1057, 2002.

Smith, A. D., The continental mantle as a source for hotspot volcanism, *Terra Nova*, *5*, 452–460, 1993.

Smith, A. D., and C. Lewis, The planet beyond the plume hypothesis, *Earth Sci. Rev.*, *48*, 135–182, 1999.

Smith, W. H. F., and D. T. Sandwell, Global seafloor topography from satellite altimetry and ship depth soundings, *Science*, *277*, 1957–1962, 1997.

Sparks, D. W., and E. M. Parmentier, The structure of three-dimensional convection beneath oceanic spreading centres, *Geophys. J. Int.*, *112*, 81–91, 1993.

Stein, C., and S. Stein, A model for the global variation in oceanic depth and heat flow with lithospheric age, *Nature*, *359*, 123–129, 1992.

Thiessen, R., K. Burke, and W. S. F. Kidd, Are African-plate topography and vulcanism simply related to underlying mantle structure?, *Eos Trans. AGU*, *58*, 503, 1977.

Thiessen, R., K. Burke, and W. S. F. Kidd, African hotspots and their relation to the underlying mantle, *Geology*, *7*, 263–266, 1979.

Thomson, K., Role of continental break-up, mantle plume development and fault reactivation in the evolution of the Gamtoos Basin, South Africa, *Mar. Pet. Geol.*, *16*, 409–429, 1999.

Turcotte, D. L., and G. Schubert, *Geodynamics: Application of Continuum Physics to Geological Problems*, 450 pp., John Wiley, New York, 1982.

Van der Beek, P., E. Mbebe, P. Adriessen, and D. Delvaux, Denudation history of the Malawi and Rukwa rift flanks (east African rift system) from apatite fission track thermochronology, *J. Afr. Geol.*, *26*, 363–385, 1998.

Vine, F. J., and D. H. Matthews, Magnetic anomalies over oceanic ridges, *Nature*, *199*, 947–949, 1963.

Wernicke, B., Low-angle normal faults in the Basin and Range Province—Nappe tectonics in an extending orogen, *Nature*, *291*, 645–648, 1981.

Wernicke, B., Uniform-sense normal simple shear of the continental lithosphere, *Can. J. Earth Sci.*, *22*, 108–125, 1985.

Wessel, P., and W. H. F. Smith, New version of the Generic Mapping Tools released, *Eos Trans. AGU*, *76*, 329, 1995.

White, R. S., and D. McKenzie, Mantle plumes and flood basalts, *J. Geophys. Res.*, *100*, 17,543–17,585, 1995.

Wolfe, C. J., and S. Solomon, Shear-wave splitting and implications for mantle flow beneath the MELT region of the East Pacific Rise, *Science*, *280*, 1230–1232, 1998.

Zhang, Y. S., and T. Tanimoto, Ridges, hotspots and their interaction as observed in seismic velocity maps, *Nature*, *235*, 45–49, 1992.

───────────

E. Bonatti, E. Carminati, and C. Doglioni, Dipartimento Scienze della Terra, Univ.à La Sapienza, P. le A. Moro 5, I-00185 Rome, Italy. (carlo.doglioni@uniroma1.it)